

Bandwidth-enhanced volume grating for dense wavelength-division multiplexer using a phase-compensation scheme

Lanlan Gu, Xiaonan Chen, Zhong Shi, Brie Howley, Jian Liu,^{a)} and Ray T. Chen^{b)}
*Microelectronics Research Center, Department of Electrical and Computer Engineering,
 The University of Texas at Austin, Austin, Texas 78758*

(Received 29 September 2004; accepted 4 April 2005; published online 25 April 2005)

A phase-compensation scheme is proposed and demonstrated to overcome the intrinsic tradeoff between the dispersion and the bandwidth of a volume grating. Its application to a volume grating-based dense wavelength-division multiplexing (DWDM) device is explored. A DWDM device is fabricated by using a 45°/82° configuration. To achieve phase compensation of the Bragg condition, a wavelength-dependent incident angle for a dispersion-enhanced holographic grating at 82° is generated through a prestaged volume hologram at 45°. The 3 dB dispersion bandwidth is increased five times by using such a device configuration. A 21-channel DWDM device centered at 1555 nm with 200 GHz spacing is demonstrated within its 3 dB bandwidth.

© 2005 American Institute of Physics. [DOI: 10.1063/1.1921333]

The volume holograms are known as a highly efficient angular dispersive element. They have been identified as an attractive solution to build wavelength-division multiplexers (WDMs).¹⁻³ Volume holographic grating-based WDMs with a surface-normal configuration, consisting of a pair of transmission volume holographic gratings and a waveguiding substrate, have been extensively investigated for their advantages of coupling and packaging.⁴⁻⁶ A schematic of a conventional device configuration is shown in Fig. 1(a). The normally incident optical signals are collimated and diffracted into a waveguiding substrate by an input grating with wavelength-dependent angles. These optical signals can be separated when traveling through the substrate with their wavelength-dependent bouncing angles. At the outputs, they are coupled out by another surface-normal volume grating with a predetermined lateral shift in the positions of their fan-outs. These spatially separated optical signals are later received by a detector array directly, or are coupled into a fiber bundle-array via a gradient index lens. For devices of this configuration, channel numbers are determined by the angular dispersion capacity, the efficiency bandwidth of the grating, and the physical size of the waveguiding substrate. However, many limitations are encountered in such a design. There exists an intrinsic tradeoff between the dispersion capacity and the efficiency bandwidth of a volume holographic grating. For the surface-normal grating described in Fig. 1(a), the dispersion capacity is proportional to $\tan \theta$, where θ is the designed diffraction angle of the grating.⁷ However, its 3 dB efficiency bandwidth is found to be approximately proportional to $1/\tan \theta$,⁸ which introduces a serious hurdle in designing a practical device. A surface-normal broadband grating with a diffraction angle at 45°, which is very close to the total internal reflection angle, was designed and fabricated for the application of dense WDM (DWDM) devices.^{4,5} However, in that structure, multiple bounces of the signal within the substrate are required to achieve enough lateral channel separation. This is due to the small angular dispersion capacity of the grating with such a small diffrac-

tion angle. The approach of multiple reflections of signal beams within a substrate will not only deteriorate the mode quality of the signals, but also broaden the beam size which increases the crosstalk between adjacent channels.

In this letter, we report a scheme to overcome this intrinsic tradeoff by generating a wavelength-dependent incident angle for a dispersion-enhanced holographic grating through a prestaged volume hologram, as illustrated in Fig. 1(b). The resultant effect is an enhancement of the demultiplexing capacity of the DWDM device. The 3 dB bandwidth of a dispersion-enhanced grating is broadened five times. Our proposed scheme is a universal solution to the intrinsic tradeoff between the dispersion capability and the efficiency bandwidth of a volume grating. Its application can also be

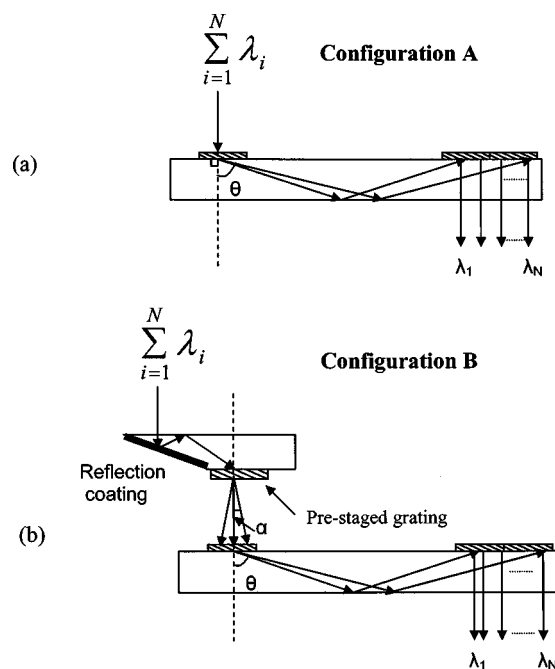


FIG. 1. Schematics of volume holographic grating-based WDMs in the surface-normal configuration. (a) Configuration A: the conventional structure. (b) Configuration B: the structure with a prestaged volume holographic grating.

^{a)}At PolarOnyx, Inc., Sunnyvale, CA 94089.

^{b)}Electronic mail: chen@ece.utexas.edu

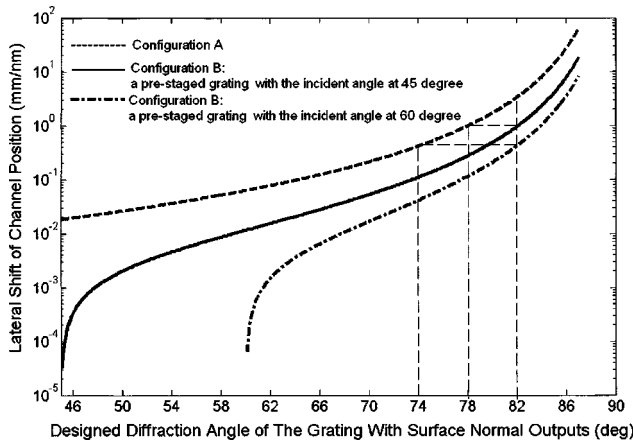


FIG. 2. Lateral shift of the channel position as a function of the designed diffraction angle of a surface-normal volume grating.

extended to other devices which are based on the dispersion of a volume grating, such as a true time delay module for a phase array antenna system.⁷

The dispersion of a volume holographic grating is given as⁹

$$\frac{\Lambda}{\sin \varphi} (\sin \alpha + \sin \theta) = \frac{m\lambda}{n}, \quad m = 0, \pm 1, \pm 2, \dots, \quad (1)$$

where Λ is the grating period, φ is the grating angle, λ is the light wavelength in vacuum, n is the refractive index of the grating material, and α and θ are the respective incident and diffraction angles of the input signal. For the conventional surface-normal configuration shown in Fig. 1(a), the diffraction angle changes with the input signal wavelength as

$$\frac{d\theta}{d\lambda} = \frac{\sin \alpha + \sin \theta}{\lambda \cos \theta}, \quad (2)$$

which can be derived from Eq. (1). For the propagation of a one-bounce distance, lateral shift in the position of the fan-outs is given by

$$\frac{dL}{d\lambda} = \frac{2d \frac{d\theta}{d\lambda}}{(\cos \theta)^2}, \quad (3)$$

where d is the thickness of the substrate. The simulation of this lateral shift is shown in Fig. 2, where a substrate thickness of 7 mm and the center wavelength at 1555 nm are used for the calculation. It is clearly shown that the lateral dispersion capacity is very dependent on the designed diffraction angle of the grating. The larger the diffraction angle, the bigger the dispersion capacity. For the conventional configuration A, the lateral dispersion increases from 0.018 to 3.3074 mm/nm when the designed diffraction angle changes from 45° to 82°. Obviously, the dispersion capacity can be enhanced by increasing the designed diffraction angle of the grating. The diffraction efficiency bandwidth of a transmission volume hologram can be simulated by using coupled wave theory.¹⁰ Simulation and experimental results of the diffraction efficiency of configuration A are shown in Fig. 3. It is clearly seen the grating passband decreases with diffraction angle. For a 82° grating, the 3 dB bandwidth only covers 8 nm centered at 1555 nm. However, for a 45° grating, less than 0.4 dB loss, with respect to the peak efficiency, occurs within a region of 40 nm. Apparently, the tradeoff

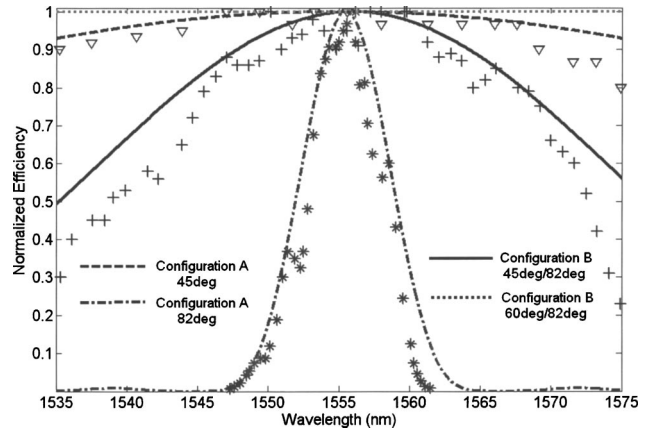


FIG. 3. Simulations and experimental results of the diffraction efficiency of the surface normal volume grating in configuration A and configuration B.

between the dispersion capacity and the efficiency bandwidth poses a huge challenge to the design of a volume grating-based DWDM device. The advantage of combining two discrete volume holograms in a 45°/82° or 60°/82° configuration is clearly indicated in Fig. 3. To achieve a broad efficiency bandwidth of a dispersion-enhanced volume grating, the incident angle of the input signal must be changed from α_0 to $\alpha_0 + \Delta\alpha$ when the input wavelength changes from λ_0 to $\lambda_0 + \Delta\lambda$. This phase-compensation condition can be derived from the Bragg condition.¹⁰ Mathematically, it is represented as

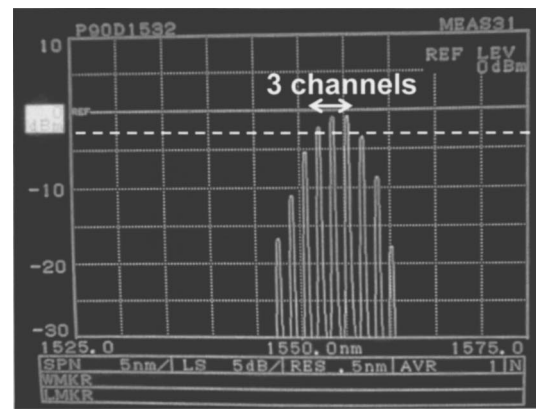
$$\frac{d\alpha}{d\lambda} = \frac{1}{2\Lambda n \cos\left(\frac{\alpha + \theta}{2}\right)} = \frac{\tan\left(\frac{\alpha + \theta}{2}\right)}{\lambda_0}. \quad (4)$$

The phase compensation for a dispersion-enhanced grating with a large diffraction angle can be achieved by using a prestaged grating. As shown by the configuration B in Fig. 1(b), an aluminum-coated beveled edge is used to change the direction of a normally incident signal to a specific incident angle for the prestaged grating. The signal at the Bragg wavelength of the prestaged grating is designed to be coupled out surface-normally. The angular dispersion of this prestaged grating provides a wavelength-dependent incident angle to the cascaded dispersion-enhanced grating that is required to achieve phase compensation. The perfect phase compensation can be achieved only when $|d\theta_1/d\lambda| = |d\alpha_2/d\lambda|$, where θ_1 is the designed diffraction angle of the prestaged grating and α_2 is the designed incident angle of the cascaded dispersion-enhanced grating. It can be calculated that, for a dispersion-enhanced grating which has a surface-normal input and a designed diffraction angle of 82°, a perfect phase compensation can be provided by a prestaged grating that has an incident angle of 60.4° and a surface-normal output. Similarly, the phase mismatch can be partially compensated by a prestaged grating which has a designed incident angle smaller than 60.4°, namely, $|d\theta_1/d\lambda| < |d\alpha_2/d\lambda|$. Both simulations and experimental data confirm the bandwidth broadening of the dispersion-enhanced grating, which is attributed to this phase-compensation scheme. In Fig. 3, simulations show the efficiency curve can be flattened significantly by using a 60.4°/82° configuration. If a 45° prestaged grating is used instead, the 3 dB bandwidth of

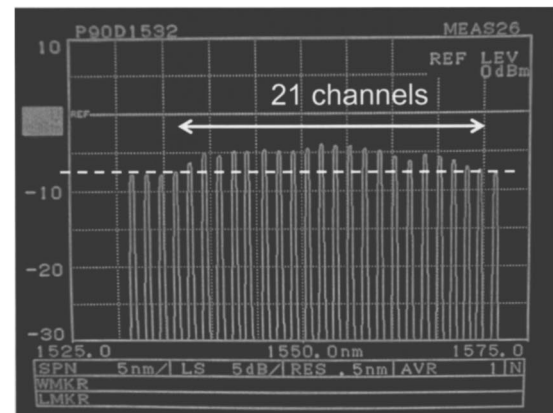
configuration B increases up to 40 nm compared with 8 nm of configuration A (without the prestaged grating). However, one side effect occurs for configuration B. The configuration with phase compensation reduces the dispersion capacity of the original dispersion-enhanced grating. The lateral channel separation for configuration B can be derived from Eq. (1) and (3). The simulation results are shown in Fig. 2. It is clearly seen, compared with the original dispersion-enhanced grating at 82° in configuration A, that the lateral channel shift decreases from 3.30 to 0.95 mm/nm and 0.42 mm/nm for configuration B with prestaged grating angles at 45° and 60.4° , respectively. However, their lateral dispersion capacities are still large, which are comparable to the original dispersion-enhanced grating with diffraction angles at 78° and 74° , where their original 3 dB bandwidths are only 12 and 18 nm, respectively. By using our $45^\circ/82^\circ$ and $60.4^\circ/82^\circ$ configurations, much broader bandwidths are achieved while the high dispersion capacity of the grating is still maintained.

To achieve DWDM channels of 200 GHz (~ 1.6 nm) spacing with low crosstalk, the $45^\circ/82^\circ$ configuration is chosen for our DWDM device considering both the efficiency bandwidth and the dispersion capacity. Its 3 dB bandwidth, which is shown in Fig. 3, covers wavelength from 1535 to 1575 nm. The 532 nm line from a 5 W Verdi laser is employed in the holographic recording. For the 45° prestaged grating, less than a 0.2 dB reduction in the channel efficiency from 1535 to 1575 nm, with respect to the peak efficiency at 1555 nm, is experimentally confirmed. The measurement results of the wavelength-dependent output angles of the prestage grating are quite consistent with the theoretical predictions. The maximum deviation angle with respect to the surface-normal direction is measured to be $\pm 0.52^\circ$ for channels at 1535 and 1575 nm. The channel efficiencies of the TE mode beam for both configuration A and configuration B are measured and plotted in Fig. 3. The experimental data and theoretical predictions are in good agreement. The output spectra for both configurations are measured by an optical spectrum analyzer, which are shown in Fig. 4. Our carefully designed configuration covers 21 channels with 200 GHz spacing within the 3 dB bandwidth while the conventional configuration can only accommodate three channels with the same spacing. More than 40 channels with 100 GHz spacing can be achieved by this DWDM device as long as the incident signals are well collimated to have a spot size smaller than $500 \mu\text{m}$ at the output. Our device has a peak efficiency of 40% and a large polarization-dependent loss (PDL). This is due mainly to the relatively low refractive index modulation (0.012) that we can achieve with Dupont photopolymer. However, simulations show that a peak efficiency of 95% and the PDL less than 0.4 dB can be achieved by our proposed structure as long as the refractive index modulation can reach 0.15 for a given photopolymer thickness of $20 \mu\text{m}$. This index modulation can easily be achieved in dichromated gelatin.¹¹

In summary, we reported a universal solution to solve the intrinsic tradeoff between the dispersion capacity and the



(a)



(b)

FIG. 4. Output spectra measured by an optical spectrum analyzer. (a) Configuration A: dispersion-enhanced grating working with a diffraction angle at 82° . (b) Configuration B: the $45^\circ/82^\circ$ configuration.

efficiency bandwidth of a volume holographic grating. By using a prestaged grating in front of a dispersion-enhanced grating, a huge enhancement of the 3 dB efficiency bandwidth can be achieved due to the phase compensation of the Bragg condition. In this work, the phase-compensation scheme is demonstrated by using the $45^\circ/82^\circ$ configuration. A 21-channel DWDM device centered at 1555 nm with 200 GHz spacing is achieved within a 3 dB bandwidth. All results are measured with a TE mode.

¹B. Moslehi, P. Harvey, J. Ng, and T. Jansson, *Opt. Lett.* **14**, 1088 (1989).

²J.-W. An, N. Kim, and K.-Y. Lee, *Jpn. J. Appl. Phys., Part 2* **41**, L665 (2002).

³J. Qiao, F. Zhao, J. Liu, and R. T. Chen, *IEEE Photonics Technol. Lett.* **12**, 1070 (2000).

⁴Y.-T. Huang, D.-C. Su, and Y.-K. Tsai, *Opt. Lett.* **17**, 1629 (1992).

⁵Y.-K. Tsai, Y.-T. Huang, and D.-C. Su, *Appl. Opt.* **34**, 5582 (1995).

⁶M. M. Li and R. T. Chen, *Opt. Lett.* **20**, 797 (1995).

⁷Z. Shi, L. Gu, Y. Jiang, H. Brie, Y. Chen, and R. Chen, *Proc. SPIE* **5363**, 39 (2004).

⁸J. E. Ludman, *Am. J. Phys.* **50**, 244 (1982).

⁹R. A. Syms, *Practical Volume Holography* (Clarendon, Oxford, 1990).

¹⁰H. Kogelnik, *Bell Syst. Tech. J.* **48**, 2909 (1969).

¹¹B. J. Chang and C. D. Leonard, *Appl. Opt.* **18**, 2407 (1979).